Synthetic autotetraploid *Caenorhabditis elegans* resist severe cold stress by escaping cold induced death at the gravid adult stage.

Laetitia Chauve[1], Aoibhin McGarry[1*], Liam Butler[1*], and Aoife McLysaght[1]

[1]Smurfit Institute of Genetics, Trinity College, Dublin

*equal contribution

ABSTRACT

Gene duplications play a major evolutionary role by providing raw material for functional innovation. Whole Genome Duplication (WGD), or polyploidization, is a particular case of duplication encompassing the entire genome and has been implicated in evolutionary diversification. In plants, WGD is recognized as a major evolutionary force, and is linked to speciation and the ability to resist periods of stress and of environmental upheaval. In animals, examples of current polyploid species are rarer, but multiple ancient events are known, including the charismatic two rounds (2R) of WGD that occurred during early vertebrate evolution. The conditions favouring the success of polyploid lineages are unclear. One debated hypothesis states that polyploidy is adaptive in the short-term, however this has never been studied in animals.

In this study, we investigated the consequences of polyploidy on physiology and stress resistance in *Caenorhabditis elegans*, where tetraploidy can be artificially constructed. Our results reveal that although tetraploidy reduces fitness by decreasing fertility and lifespan in regular conditions, tetraploid animals exhibit increased resilience under specific stress conditions related to temperature changes. While neotetraploid animals exhibit similar pathogen resistance, their response to heat stress is altered. They exhibit modest improvement in thermotolerance and prolonged *hsp* (heat shock protein) mRNA induction upon heat shock (HS) accompanied by altered *hsp-16.2* nuclear localization upon HS. Most notably, under severe cold stress, gravid neotetraploids animals massively escape cold-induced death, and generate more progeny than diploid animals. These results suggest a potential adaptive value of tetraploidy under cold stress and might help explain recent correlations found between

the frequency of extant animal polyploids and regions experiencing recent glaciation and large temperature variation.

INTRODUCTION

Whole genome duplication (WGD), or polyploidization, is an unusual event where the entire genetic sequence becomes repeated within the nucleus of the cell. WGD can arise either from hybridization between genomes of two related species (allopolyploidization), or from doubling the entire set of chromosomes in the same taxon, usually due to an error during meiosis (autopolyploidization). WGD is a major evolutionary force that has had profound and lasting effects on the genomes of animals, plants and protists (Van De Peer, Mizrachi, and Marchal 2017). Duplication, be it small-scale duplication (SSD) or WGD, may play a major role in evolution by providing raw material for functional innovations. Nevertheless, WGD differs from SSD as it allows the duplication of dosage sensitive genes (Birchler et al. 2005).

WGD events have been identified in most eukaryotic lineages (Wolfe 2015). Polyploidy is common in plants, where it has been linked to speciation events, and the ability to withstand periods of stress It is estimated that 35% of extant plants are polyploids (David 2022). In allopolyploids, it may be advantageous to bring together the best of two different genomes, a phenomenon known as hybrid vigour or heterosis. Nevertheless, autopolyploidization in plants is also associated with increased abiotic stress resistance (Del Pozo and Ramirez-Parra 2014) and resistance to pathogens (Mehlferber et al. 2021; W. Wang et al. 2018). It is estimated that about half of the WGD events in angiosperms originate from autopolyploidization (Barker et al. 2016).

Polyploidy is rarer in animals, with an estimated frequency of less than 1% across animals (Ryan Gregory and Mable 2004; Otto and Whitton 2000). Polyploidy is almost absent in birds and mammals where it is not well tolerated, and extant animal polyploids belong to amphibians, insects, arachnids, molluscs, fishes and nematodes (David 2022). However, we know of two ancient rounds of WGD that occurred during early vertebrate evolution; one of these is shared by all vertebrates, and the second by all jawed vertebrates (gnathostomes) (Nakatani et al. 2021; Simakov et al. 2020). An additional WGD occurred at the base of teleost fish (Jatllon et al. 2004). Generally, WGD is followed by a period of extensive gene loss and rediploidization, processes

which reshape the genome and channel evolutionary outcomes, and a large fraction of genes in descendent lineages are duplicates that can be traced back to this event (an estimated 20-30% of protein coding genes in humans (Makino and McLysaght 2010; Nakatani et al. 2007)).

The WGD events that have been well-studied are generally very ancient and little is known about the short-term or immediate consequences of polyploidization on the genome and on physiology in metazoans. Polyploidy is a relatively common mutational event, but rare over evolutionary times (i.e., it is usually an evolutionary 'dead end'). What factors contribute to the success of a polyploid lineage remain unknown, particularly in animals. One attractive though controversial hypothesis states that polyploidy might increase tolerance to stressful environments and be adaptive on the short-term (Van de Peer et al. 2021).

It is well established that stress itself (i.e. heat or cold) can lead to autopolyploidy via the generation of unreduced (i.e. diploid) gametes by failure of germline cell division after meiotic replication (Ryan Gregory and Mable 2004). Therefore, a legitimate question is whether autopolyploidy might have an adaptive value under stressful conditions or whether it is merely a consequence of the stress. Studies in yeast show that increasing ploidy can be beneficial under specific stress conditions (Harari et al. 2018). Furthermore, experimental evolution studies indicate that populations of autotetraploid yeast fix beneficial mutations faster than diploids (Selmecki et al. 2015), and despite being initially more sensitive to growth temperature, evolved tetraploid yeast become more robust to high temperatures (Lu, Swamy, and Leu 2016). WGD events in plants are correlated with periods of climatic changes and unstable environments (Van De Peer, Mizrachi, and Marchal 2017; Van de Peer et al. 2021), and it has also been suggested to be the case for amphibians and fish (Mable, Alexandrou, and Taylor 2011). Indeed, the distribution of Australian autotetraploid burrowing frog *Neobatrachu*s suggests that autotetraploids are better adapted to harsher environments (Van De Peer, Mizrachi, and Marchal 2017). Recent work revealed higher genetic diversity in autotetraploid *Neobatrachus* and better adaptation to recent climate changes due to polyploidy mediated gene flow (Novikova et al. 2020).

Autopolyploidy also exists at the tissue or organ level (somatic polyploidy), such as in the placenta, liver, heart, skin and mammary gland cells in humans (Schvarzstein et al. 2023). Somatic polyploidy has also been associated with stress resistance. Environmental stresses such as viral infections (Li et al. 2018) and wound healing (Losick, Fox, and Spradling 2013) trigger somatic polyploidy. Furthermore, polyploidy protects the liver against hepatotoxic stress (Sladky et al. 2021; Lin et al. 2020). Additionally, cell polyploidy is a hallmark of many cancers where increased ploidy is observed in many different types of tumours, and participates in tumour initiation and resistance to treatment (Was et al. 2022). .

To investigate whether autopolyploidy has an adaptive value in the short-term in animals, we sought to investigate the consequences of induced autopolyploidy on physiology and stress responses in the nematode *Caenorhabditis elegans. C. elegans* was the first metazoan where stable tetraploid lines could be established in 1949 by Nigon after exposing *C. elegans* to repeated heat stress or exposure to colchicine, and screening for animals with longer body size (Madl and Herman 1979). The karyotype of neotetraploid animals was checked by visualizing chromosome bivalents in late oocytes at the diakinesis stage. More recently, a protocol has been established to rapidly generate synthetic autotetraploid *C. elegans* from almost any genetic background, by transiently knocking-down the cohesin complex component *rec-8* by RNA interference for two generations (Clarke et al. 2018). *C. elegans* provides several advantages as a model to study the consequences of polyploidy (Schvarzstein et al. 2023). Derived tetraploid animals lines are stable (siring mostly tetraploid animals) and fertile enough to work with. With its mostly self-fertilizing hermaphrodite mode of reproduction it provides isogenic genetic backgrounds for comparison, differing only by ploidy levels.

The study of tetraploid *C. elegans* lines helped understand sex chromosome composition and sex determination (Madl and Herman 1979), and provided insight into meiosis in a tetraploid context, revealing a biphasic model where homologous chromosomes are first grouped together before pairwise synapsis associations are established (Roelens, Schvarzstein, and Villeneuve 2015). As shown in other polyploid organisms, neotetraploid animals exhibit an increase in body size, estimated to about 40% increase in volume at the late L4 (larval 4) stage (Lozano et al. 2006). During the development of normal diploid *C. elegans*, intestinal and hypodermal cells become

polyploid, and it has been shown that tetraploidy controls body size by controlling somatic polyploidy in the epidermis via TGFβ-signalling and cyclin-1 (Lozano et al. 2006). However, the impact of unscheduled autotetraploidy on other physiological aspects and in the context of stress is unknown.

Here we generated autotetraploid animals using the *rec-8* RNA interference protocol (Clarke et al. 2018) and exposed synthetic tetraploids to various stresses. We show that unscheduled autotetraploidy is deleterious under regular growth conditions: neotetraploids have a shorter lifespan and decreased fertility. Consistent with previous reports, we find that neotetraploids are bigger at late L4 stage/young adult stage. However, we report here that this is not always true as animals age. At day two of adulthood, the body size of neotetraploids is no longer increased compared to wild-type (WT) diploid animals, a process that seems independent of TGF-β signalling. Exposing neotetraploid *C. elegans* to stressful environments revealed altered phenotypes under specific stress conditions related to temperature changes. While neotetraploids exhibited similar survival on pathogenic bacteria, they displayed a modest increase in heat stress resistance, with an altered kinetics of *hsp-16* molecular chaperones induction, accompanied by an altered nuclear localization of *hsp-16.2* DNA locus. When exposed to severe cold stress followed by recovery, gravid neotetraploid animals massively escaped cold-induced death. Additionally, following cold stress, neotetraploids produced more progeny than their diploid counterparts, suggesting potential adaptive value of autotetraploidy under cold stress conditions.

RESULTS

Fitness of tetraploids decreased under regular conditions

To assay the physiological consequences of unscheduled autopolyploidy in *C. elegans*, we generated neotetraploid animals using *rec-8* RNA interference (Clarke et al. 2018). We obtained stable lines siring almost exclusively tetraploid animals, with only rare events of reversion to diploidy. Tetraploids were selected in the F2 progeny based on body-size increase (Madl and Herman 1979; Clarke et al. 2018). We confirmed polyploidy status by checking for doubling of chromosome bivalents in late-stage oocytes at diakinesis stage (**Figure 1A**), similarly to (Clarke et al. 2018).

Phenotypic characterization under regular growth conditions (20°C) showed that neoautotetraploid animals are developmentally delayed (**Figure 1 B-C**) exhibiting more stage heterogeneity at 65h post egg-laying synchronization than diploids. The delay in reaching adulthood for the majority of tetraploid animals is estimated to be between 8-10h at 20°C. Further analysis showed that neotetraploids exhibit a higher rate of embryonic lethality (between 7-9%) than diploids (around 1%) (**Figure 1C**). Autopolyploidization severely affected their number of progeny, which is now reduced to 28.5% of WT progeny. Furthermore, lifespan was significantly decreased in two independent lines of neoautotetraploids at 20°C. Altogether, these results show that, under regular growth conditions, unscheduled autopolyploidization has deleterious consequences on fitness and negatively affects development, fertility and lifespan.

Body-size increase in tetraploid does not maintain during aging

Autopolyploidization is associated with body size increase in *C. elegans* (Lozano et al. 2006). However, body size measurement were carried out exclusively at the young adult stage, after the L4/young adult moult, after the vulva has been everted. We characterized body volume changes during development (**Figure 1G**) and during adulthood (**Figure 1H**) for diploids, derived tetraploids and *dbl-1(nk3)* loss of function mutants as a negative control. As shown in **Figure 1F**, our analysis revealed that while neotetraploids are bigger than diploids during development, with a 37% increase in length (**Figure S1A**) and an about 80% increase in body volume (**Figure 1H**) at the late L4 stage, this increase in body size is not maintained as animals progress during adulthood. Twenty-four hours after late larval stage L4/young adult, as animals enter the second day of adulthood and are now gravid, their body size is increased by only 10% in length (**Figure S1A**) and is decreased by 12 % in volume (**Figure 1H**) compared to diploid animals. From day 2 of adulthood on, the body size of tetraploids remains similar in length to that of diploids, and their volume stays smaller than diploids. In day 2 gravid adults, the decrease in volume, but not in length of tetraploids might be due to the tri-dimensional impact of width differences due to the gonad of tetraploids carrying fewer embryos than diploids.

DBL-1, the ligand of the neuroendocrine TGF-ß/BMP signalling pathway, is known to control body size in a dose-dependent manner (Gumienny and Savage-Dunn 2013; Lozano et al. 2006; Flemming et al. 2000). As expected, the body size of *dbl-*

1(nk3) loss of function mutants was decreased in volume throughout development and adulthood (**Figure 1G-H**). In a neotetraploid context, as investigated at the late L4/young adult stage, DBL-1 regulates body size by controlling the somatic ploidy of the hypodermis (Lozano et al. 2006). We noticed that the ratios of body volume increase between L4 and day 2 adults were similar in neotetraploids compared to *dbl-1(nk3)* loss of function mutants, at about 2 fold, whereas the volume of diploids increased by about 4 fold (**Figure 1I**). We therefore hypothesized that, in neotetraploids, a decrease in the activity of TGF-ß signalling pathway from the day 2 stage onwards could be responsible for slowing down the body size increase. However our analysis of TGF-ß/BMP signalling transcriptional activity by monitoring steady state mRNA levels for *dbl-1*, downstream TGF-ß/BMP signalling upregulated target genes (*sma-3 sma-4, sma-6*), positive regulator *sma-10,* and negative regulators *lon-1* and *lon-2,* displayed no significant difference between diploids and tetraploids at either L4 stage of day 2 adult stage for any of those genes (**Figure S1B-H**). This suggests that a change in TGF-ß/signalling activity is not the reason underlying the slowdown of body size increase in tetraploids from day 2 stage on.

The dynamics of the heat stress response is altered in tetraploids

While unscheduled autotetraploidy negatively affects lifespan under regular growth conditions at 20°C (**Figure 1J**), there was no deleterious effect on lifespan under conditions of mild heat stress at 25°C (**Figure 1K**). The lifespan of one of the neotetraploids line (MCL2 4n #2) was even slightly improved compared to diploid control, although not significantly (**Figure 1K**). The improvement in lifespan of neotetraploids with increasing temperature prompted us to assess the heat stress response in neotetraploids. The heat stress response is a highly conserved response relying on the transcriptional activation of molecular chaperones (also called *heat shock proteins (hsps)*) upon heat stress in order to maintain and restore cellular protein homeostasis (Lindquist 1986). The transcription factor heat shock factor-1 (*hsf-1*) is the master regulator of molecular chaperones and is known to be involved in the regulation of lifespan in a temperature dependent manner, with an increased contribution at elevated temperatures (Douglas et al. 2015; Chauve et al. 2021; Lee and Kenyon 2009). After exposure to severe heat stress (thermorecovery), neotetraploids animals raised at either 20°C or 25°C exhibited a modest increase in survival (p-value ploidy effect =0.0070, **Figure 2A**).

Molecular chaperones are comprised of several gene families, some of which are constitutively expressed (i.e. *hsp-1, hsp-90*), while others are expressed at low levels under normal conditions and highly induced and attenuated following heat shock (*hsp-16* small *hsp* family and *hsp-70*(C12C8.1)). We monitored the kinetics of induction of highly inducible *hsps* following a short heat shock pulse (30 min at 34°C) for the highly inducible molecular chaperones *hsp-16.1* and *hsp-16.2* by quantitative Real Time PCR (qRT-PCR). Our analysis revealed delayed kinetics in the transcriptional activation and attenuation of *hsp-16.1* and *hsp-16.2* upon heat shock (**Figure 2B**). While hsp-16.1 and hsp-16.2 mRNA levels had returned to basal levels in diploids at four hours after heat shock, mRNA levels remained elevated in two independent lines of neotetraploids.

How can tetraploidization affect the kinetics of induction of molecular chaperones? We hypothesized this phenomenon could be linked to altered positioning relative to the nuclear envelope, as the *hsp-16.2* DNA locus is located in proximity of the nuclear envelope and of the nuclear pore, for rapid mRNA export upon heat shock (Rohner et al. 2013). Yet polyploidy alters the ratio of the nuclear envelope surface to nuclear volume. Indeed, the volume of the nucleus is doubled while the nuclear envelope is only increased by 1.6 fold (Doyle and Coate 2019). To explore this, we generated neoautotetraploid animals carrying the in-vivo tracking system for the *hsp-16.2* DNA locus: *hsp-16.2p*::LacO/*baf-1p*::GFP-LacI (Rohner et al. 2013). As depicted in **Figure 2C**,**2F**, we measured nuclear positioning of *hsp-16.2* loci relative to the nuclear envelope in early embryonic (~50 cell stage) nuclei by classifying the position of each *hsp-16.2* locus into three zones of equal surface within the nuclear plane, (**Figure 2F**) according to (Meister et al. 2010). This analysis showed that tetraploidy does not affect *hsp-16.2* DNA locus positioning relative to the nuclear envelope in the absence of heat shock (p-value diploid vs tetraploid =0.5715 in **Figure 2D**, Chi-square three zones p-value =0.8638, **Figure 2G**). However, following a short pulse of heat-shock (10 minutes at 34°C), hsp-16.2 loci were more frequent in zone 1 and more closely associated with the nuclear envelope (p-value diploid vs tetraploid =0.0204 in **Figure 2E**, Chi-square: p-value =0.0019, **Figure 2H**). Altogether, these data suggest that the delayed kinetics in transcriptional activation of highly inducible *hsps* upon heat shock could be linked to changes in nuclear geometry and architecture caused by tetraploidization.

Contrasting results using proteostasis sensors suggest that the behaviour of multicopy transgenes is changed in tetraploids

As an alternative approach to investigate the consequences of autotetraploidy on proteostasis capacity, we generated tetraploid animals carrying the proteostasis sensor *unc-54p::*Q35::YFP, a multicopy transgene carrying stretches of polyglutamine (polyQ) expansion repeats fused a fluorophore, and expressed in muscles. This transgene is used to monitor proteostasis capacity in muscles, by visualisation of polyglutamine aggregates when proteostasis capacity is compromised (Morley et al. 2002). As shown in **Figure S2A-C**, neotetraploid animals carrying *unc-54p::*Q35::YFP exhibited a marked increase in Q35 aggregation at both temperatures assayed (20°C and 25°C) at day 2 of adulthood, indicative of reduced protein folding capacity in muscles. These data contrast with previous results showing a modest increase in thermorecovery of tetraploids at both 20°C and 25°C (**Figure 2A**), suggesting a modest increase in proteostasis capacity of tetraploids at the whole animal level, when they do not carry any multicopy transgene. We investigated endogenous mRNA levels for several constitutive molecular chaperones in the presence or absence of the multicopy unc-54::Q35:YFP transgene. While levels were globally unaffected by ploidy in the absence of the Q35::YFP transgene (p-value ploidy effect=0.2232), molecular chaperone levels were globally higher in animals carrying Q35::YFP (p-value ploidy effect=0.0086) with the highest effect observed on the endoplasmic reticulum (ER) chaperone *hsp-4* (p-value=0.0679), a sign of ER stress. Q35::YFP is a highly expressed mutlicopy transgene (see difference in scale in **Figure S2E**), and its levels seemed higher in tetraploids (even if not significantly so). It is possible that higher levels of this transgene in tetraploids are negatively affecting cellular protein folding capacity. To determine if proteostasis capacity was also affected by the expression of multicopy transgenic proteostasis sensors in other tissues, we tetraploidized animals carrying *vha-6p*::Q44::YFP, expressed in the intestine. At day 4 of adulthood neotetraploids also exhibited a significant increase in intestinal Q44 aggregation at 20°C in two independent lines (**Figure S2F-I**). To disentangle the effects of multicopy transgenic proteostasis sensors on protein folding capacity in neotetraploids, we assayed proteostasis capacity in muscles in the absence of any multicopy transgene, using the *unc-54(e1301)* temperature sensitive (ts) mutation in heavy-chain myosin with phenotypic consequences in muscles. In *unc-54* ts mutants, a decrease in protein

folding capacity is correlated with motility defects. Our results indicate that tetraploidy does not affect the motility of *unc-54(e1301)* mutants (p-value ploidy effect=0.7110), but there is an interaction between temperature and ploidy (p-value interaction=0.0276) with a slight decrease in motility at 15°C (**Figure S2I**) and a small improvement at 25°C (**Figure S2K**). Altogether, these results suggest that tetraploidy affects multicopy transgenes, possibly by affecting their regulation. This leads to a decrease in protein folding capacity.

Tetraploids exhibit similar resistance to pathogenic bacteria

In plants, auto-polyploidy confers resistance to pathogenic bacteria, by constitutively activating plant defences (Mehlferber et al. 2021; Saei et al. 2018) and modelling approaches predict better resistance of polyploids to pathogens and parasites (Oswald and Nuismer 2007). By contrast, synthetic triploid rainbow trout and Atlantic salmon are more susceptible to viruses, bacteria and parasites (Zhou and Gui 2017). We sought to test the resistance of synthetic *C. elegans* tetraploids to its most studied pathogen, *Pseudomonas aeruginosa*. *P. aeruginosa* is an opportunistic pathogen of animals, insects, nematodes and plants. *P. aeruginosa* kills *C. elegans* in several ways, depending on the environment (Kirienko et al. 2014; Scott et al. 2020). Under conditions of low osmolarity, *P. aeruginosa* colonizes the intestine and kills nematodes within a few days (slow killing assay).

We monitored resistance to pathogenic bacteria in animals of different ploidies using *P. aeruginosa* strain PAO1. As exposure to *P. aeruginosa* leads to matricide "bagging" phenotype in gravid adults, we performed the experiments in sterile nematodes, either upon exposure to 5-Fluorodeoxyuridine (FuDR) which inhibits cell divisions in the progeny (**Figure 2I**), or using the gonadless temperature sensitive genetic background *gon-2(q388);gem-1(bc364)* (Kemp et al. 2009) (**Figure 2J**). We observed similar resistance of neotetraploids compared to diploids under both conditions (**Figure 2 I-J**), suggesting that autotetraploidy does not alter the response to pathogenic *P. aeruginosa* in *C. elegans*.

Gravid adult tetraploids escape cold-induced death under severe cold stress

The frequency of polyploid plants correlates with higher latitudes and regions of colder climate (Rice et al. 2019). Several studies have demonstrated that autopolyploidization is associated with increased tolerance to cold in plants both in

wild polyploid populations adapted to cold environments (Syngelaki, Paetzold, and Hörandl 2021) or under induced autopolyploidization (Y. Jiang et al. 2020; Deng et al. 2012). The response to cold stress has been less extensively studied than the heat stress response. Nevertheless, in the last decade several studies showed that severe cold induces cold-stress induced genetically programmed death, or phenoptosis, more prominently in adults than larvae (W. Jiang et al. 2018). This cold-induced death is thought to be an adaptive strategy to promote kin selection at the population level by favouring younger hermaphrodites more fit for reproduction (W. Jiang et al. 2018). Recent work showed that exposure to severe cold stress in gravid adults promotes lipid relocalization from the intestine to the germline, as a proposed terminal response investment to allocate resources to the progeny at the detriment of parental survival (Gulyas and Powell 2022). This cold-induced reproductive response depends on neuronal sensation of cold temperature through TAX-2/TAX-4 cGMP gated channels expressed in a subset of sensory neurons, which triggers lipid relocalization into embryos via vitellogenin lipid transporters (Gulyas and Powell 2022).

We assayed resistance to a severe cold stress in neotetraploid animals. Plates containing worms were places in an box of ice for four hours, followed by 20 hours recovery at 20°C (**Figure 3A**). While ploidy did not significantly affect survival after cold recovery at the L4 stage (**Figure 3B**), there was a dramatic difference in gravid adults at day 2 of adulthood. Diploid day 2 adults massively died (~2% survival) while 80-95% of day 2 adult tetraploid survived (**Figure 3B**). At the time of scoring, the matricide “bagging” phenotype was observed in day 2 adult diploids. To ensure death of diploids was caused by exposure to cold rather than by internal hatching, we performed the cold recovery assay in day 2 adults using FuDR. We could still detect a significant difference in survival, although FuDR improved survival of diploids to 20-40% survival (**Figure 3C**). We found that cold-induced death at day 2 of adulthood depends on the presence of a fully functional gonad, as temperature sensitive gonadless diploid *gon-2(q388);gem-1(bc364)* mutants survived cold recovery as day 2 adults at a similar rate than neotetraploids, recapitulating previous results in *glp-1* sterile diploids exposed to cold-shock (Gulyas and Powell 2022).

Recovery from severe cold stress is affected by cold acclimation at lower growth temperature (15°C) (Ohta et al. 2014). Cold acclimation is controlled by neuron-intestine hormonal signalling from a subset of thermosensory head neurons

(Ohta et al. 2014; Okahata et al. 2022). Under growth at lower temperature, neuroendocrine I nsulin and steroid hormone signalling from the ASJ neuron leads to the activation of insulin signalling in the intestine and lipid composition changes promoting cold resistance (Okahata et al. 2022). We assayed cold recovery at different growth temperatures. While growth at 25°C resulted in a similar phenotype as observed at 20°C, cold acclimation at 15°C promotes close to 100% survival after cold recovery in a similar manner in diploids and tetraploids, at both L4 and day 2 adult stage (**Figure 3E**).

Cold shocked tetraploids produce more progeny of similar quality compared to diploids

Fertility is strongly compromised in neotetraploids under normal conditions. As neotetraploid gravid adults escape cold-induced death, we wondered how the output number of progeny of cold-shocked neotetraploids would compare to the progeny of cold-shocked diploid animals upon recovery from severe cold stress. Our analysis revealed that the overal number of progeny of cold-shocked tetraploids is 2 fold higher than the progeny of cold-shocked WT diploids, suggesting a potential adaptive advantage of neotetraploidy at the population level under cold stress conditions (**Figure 3F**). In cold-shocked diploids, the average number progeny is reduced by about 10 fold compared to non cold-shock (**Figure 1E** and **Figure 3F**), with the progeny coming from eggs laid within 0 to ~5h hours after the end of cold shock and from internal hatching when P0 diploids die around 10-12h post cold shock. In tetraploids, the average number of progeny following cold shock is reduced by about 2 fold compared to non cold shock conditions (**Figure 1E** and **Figure 3F**).

Cold-induced death is proposed as a terminal investment response to favour progeny to the detriment of parents, with the progeny of cold-shocked diploids resisting better to cold shock (Gulyas and Powell 2022). We sought to determine whether the progeny of cold-shock tetraploids, which escape cold-induced death, might exhibit decreased fitness compared to the progeny of cold-shock diploids. Upon recovery from cold shock, progeny were collected at different time points after cold shock (**Figure 4A**). Embryonic lethality was severely increased in the F1 progeny of cold shock animals (**Figure 4B**), however, neotetraploid F1 animals were slightly less affected (p-value ploidy = 0.0504). As a another measure of fitness, we assayed

developmental stage of synchronized F1 progeny from P0 at either 0h or 3h post cold shock (when P0 diploids were still alive). As tetraploids are developmentally delayed compared to their diploid counterparts (**Figure 1B-C**), we compared the stages of cold-shocked progeny to non-cold shocked animals of the same ploidy. At 0h post cold shock, the developmental index of both cold shocked diploids and tetraploids was reduced (**Figure 4D**). F1 progeny of diploids and tetraploids were similarly developmentally delayed upon cold shock (p-value = 0.3014) (**Figure 4E**). At 3h post cold shock, the developmental index of tetraploids seemed slightly less reduced than for diploids (**Figure 4F**), but the developmental delay was overall not different with ploidy (**Figure 4G**). We then exposed the progeny of cold shocked P0 animals of different ploidies collected at different time points to a cold-shock at the L4 stage, however, we could not detect any difference in survival of the progeny between the two ploidies (**Figure 4C**). Altogether, these data indicate that gravid neotetraploids escape cold-induced death and produce twice as many progeny than diploids following cold shock. The fitness of the progeny of neotetraploids is similar if not slightly better compared to the progeny of their diploids counterparts.

DISCUSSSION

Whether induced autopolyploidy might be beneficial for a multicellular animal in a stressful environment is a current matter of debate. In this study, we explored the consequences of induced autotetraploidy on physiology and investigated how it affects stress responses in the nematode *C. elegans*. While this manuscript was in preparation a pre-print study was released that investigated the consequences of autotetraploidy in *C. elegans* on physiology and response to chemotherapeutic drugs (Misare et al. 2023). Our study is, however, the first one to investigate stress responses to heat, cold and pathogens in a synthetic autotetraploid multicellular animal.

We show, that under regular conditions, induced autotetraploidy has deleterious consequences on fitness. Neoautotetraploids are developmentally delayed, short-lived and their fertility is reduced by about 71% compared to diploids. These results recapitulate recent findings of (Misare et al. 2023). There is consensus that polyploidy is generally associated with an increase in body size in invertebrates,

but not in vertebrates (Doyle and Coate 2019) where polyploidy can sometimes lead to an increase in cell size accompanied by a reduction in the overall number of cells (Cadart et al. 2023). Previous studies in autotetraploid *C. elegans* report a body size increase of ~30% at the lateL4/young adult stage (Lozano et al. 2006; Misare et al. 2023). Our own measurements of body size throughout life, however, reveal for the first time that this increase in body size compared to diploid is not maintained throughout life, falling from day 2 of adulthood on. We show that this is not linked to a change in TGF-ß/BMP signalling activity between L4 and Day 2 of adulthood in neotetraploids. The molecular mechanisms underlying this phenomenon remain to be elucidated, and one hypothesis could be a link with deleterious effects of tetrapolyploidy in the germline. Indeed day 2 of adulthood marks the starts of embryonic production, and the germline of autotetraploid *C. elegans* has been recently associated with increased apoptosis (Misare et al. 2023).

In contrast to autopolyploid plants, exposure to pathogenic bacteria did not lead to an altered response in neotetraploid *C. elegans*. Exposure to heat stress revealed a modest increase in thermorecovery, with a delayed kinetics of *hsp* transcriptional induction upon heat shock. It is possible that the latter is linked to nuclear architecture changes caused by the change in the ratio of the nuclear envelope surface to nuclear volume, as suggested by our in-vivo tracking of the *hsp-16.2* DNA locus within the nucleus. Severe cold stress followed by recovery revealed that gravid neotetraploid animals are able to escape cold-induced death. Following severe cold stress, they produce twice as many progeny of similar fitness compared to their cold-shocked diploid counterparts. The fact that survival after cold recovery is not altered at the L4 stage suggest that the intrinsic cold resistance capacity of neotetraploids is not altered, and that the phenotype is linked to genetically programmed death in gravid adults.

The molecular mechanisms underlying cold-induced death escape in gravid adults remain to be elucidated. One path of interest will be to investigate whether the genetic program responsible for cold-induced death is altered in neotetraploids. Upon recovery from severe cold, the transcription factor ZIP-10 is upregulated, leading to activation of several proteases and triggering organismic death (W. Jiang et al. 2018). ZIP-10 is regulated by ISY-1 and the micro RNA *mir-60*. In addition, neuronal signalling is known to play a role, as cold induced death requires functional TAX-2/TAX-4 cGMP receptor signal from a subset of thermosensory neurons (Gulyas and Powell 2022)

and the G-coupled protein receptor FSHR-1 is also an identified mediator of cold-induced programmed death (C. Wang et al. 2023). Ultimately, alterations in lipid metabolism in the intestine, and lipid relocalization from the intestine to the germline upon cold recovery require further investigation.

Our study reveals that induced autotetraploidy alters responses to temperature related stresses, and that gravid autotetraploid *C. elegans* escape cold-induced death with potential adaptive consequences at the population level. This work may help explain recent results showing a strong geographical correlation between the frequency of wild polyploids of three clades (Amphibia, Actinopterygii, and Insecta) and regions experiencing recent glaciation and large variation in temperature (David 2022).

ACKNOWLEDGEMENTS

We are grateful to Professor Marie-Anne Felix and Professor Henrique Teótonio from Institut de Biologie de l'Ecole Normale Superieure (IBENS) de Paris for helpful discussions. We are thankful to Dr Carsten Kröeger from the Microbiology Department at Trinity College for help with the *Pseudomonas aeruginosa* experiment. We would like to thank Dr Gavin McManus from the School of Biochemistry and Immunology Imaging facility at Trinity College, Dr Kartsen Hokamp from the bioinformatics facility in the Genetics Department at Trinity College and Dr Pablo Labrador in the Genetics Department at Trinity College for all their help. We thank the Caenorhabditis Elegans Center (CGC) for providing some strains. The CGC is funded by NIH Office of Research Infrastructure programs (P40 OD010440). This work was supported by funding from the European Research Council, grant agreement 771419, and from Science Foundation Ireland.

LIST OF SUPPLEMENTARY INFORMATION

Figure S1- The transcriptional activity of TGF-β/BMP signalling pathway is similar between tetraploid and diploid animals at either L4 stage or Day2 of adulthood.

Figure S2- Contrasting results obtained using different proteostasis sensors suggest a change in the behaviour of multicopy transgenes in tetraploid animals.

Table S1- Primers used for quantitative Real Time PCR

GENERAL METHODS

C. elegans maintenance

Nematodes were grown on NGM plates seeded with *Escherichia coli* OP50 strain at 20°C unless otherwise stated, according to standard methods (Brenner 1974).

List of *C. elegans* strains

To distinguish between the genotypes of diploid and tetraploid worms, the following nomenclature was used, similar to (Clarke et al. 2018). The number of autosomal chromosomes is listed as 2A in diploid and 4A in tetraploid animals. Neotetraploid hermaphrodites can carry either 3X or 4X chromosomes (Madl and Herman 1979; Nigon 1949), with “allélogènes” 4A:3X siring 40% males in their progeny while “thélygènes” 4A:4X hermaphrodites exhibit 0.7% males in their progeny. All the derived tetraploid lines generated here carry 4X chromosomes, based on male frequency in their progeny.

The following strains were used: N2 (2A:2X) WT, AM140 (2A:2X) *rmIs132* [*unc-54p*::Q35::YFP], AM738 (2A:2X) *rmIs297* [pAMS66 *vha-6p*::Q44::YFP + *rol-6(su1006)* + pBluescript II], CB1331 (2A:2X) *unc-54(e1301)* I temperature sensitive, EJ1171 (2A:2X) *gem-1(bc364); gon-2(q388)* temperature sensitive, GW615 (2A:2X) *gwSi3* [*hsp-16.2::wmCherry; 256x LacO; unc-119(+)]; gwIs39[baf-1::gfp-LacI::let-858 3’UTR; vit-5::gfp*] III; *unc-119(ed3)* III, NU3 (2A:2X) *dbl-1(nk3)* V.

The following strains were generated. Tetraploid derivative of N2: MCL1 (4A:4X) WT line #1, MCL2 (4A:4X) WT line #2. Tetraploid derivative of AM140: MCL6

(4A:4X) *rmIs132* [*unc-54p*::Q35::YFP]. Tetraploid derivative of GW615: MCL7 (4A:4X) *gwSi3* [*hsp-16.2::wmCherry; 256x LacO; unc-119(+)]; gwIs39[baf-1::gfp-LacI::let-858 3'UTR; vit-5::gfp*] III; *unc-119(ed3)* III. Tetraploid derivatives of AM738: MCL20 (4A:4X) *rmIs297* [pAMS66 *vha-6p*::Q44::YFP + *rol-6(su1006)* + pBluescript II] line #1, and MCL21 (4A:4X) *rmIs297* [pAMS66 *vha-6p*::Q44::YFP + *rol-6(su1006)* + pBluescript II] line #2. Tetraploid derivative of EJ1171: MCL22 (4A:4X) *gem-1(bc364); gon-2(q388)* temperature sensitive. Tetraploid derivatives of CB1331: MCL25 (4A:4X) *unc-54(e1301)* I temperature sensitive line #1, and MCL26 (4A:4X) *unc-54(e1301)* I temperature sensitive line #2.

Generation of tetraploid *C. elegans* strains

Autotetraploid strains were generated by RNA interference of the cohesin component complex *rec-8* for two generations and selection of longer worms in the F2 progeny (Clarke et al. 2018). Longer worms were passed for a few generations, typically 3-10, before stable lines siring only tetraploids were obtained. Occasionally, diploid revertant worms were observed.

Worm synchronization

Worms were synchronized by egg-laying of several 6 cm plates each containing 20-30 gravid adult worms for diploids and about 60 gravid adults for tetraploids. Gravid adults were then removed and the progeny were assayed at the indicated time post synchronization. For experiments involving the gonadless mutant *gon-2(q388);gem-1(bc364)*, gravid adults were synchronized for 12-14h at the permissive temperature (15°C). Gravid adults were removed and nematodes were then switched to the restrictive temperature (25°C). Nematodes were then selected at late L4 larval stage.

Body size measurements

For experiments during development, worms were assayed at the indicated hours post egg-laying synchronization. For experiments during adulthood, worms were all selected based on the late L4 stage (Mok, Sternberg, and Inoue 2015), and nematodes were transferred every day until day 5 of adulthood. Animals were paralyzed in 3mM Levamisole diluted in M9, and mounted on a 2% agarose pad. The length and width of each individual worm was measured using FIJI/ImageJ (Schindelin

et al. 2012). Volume was estimated from length and width measurements, considering worms as a cylinder.

Fertility assay

About 20 worms per condition were singled out in 12-well plates seeded with 50-µL OP50 at the L4 stage. Each day, all animals were passed onto new 12-well plates. The F1 progeny laid by each individual P0 worm was scored 2 to 3 days after the parent worm had been transferred to the well, when the F1s were either L4 or adults. For fertility experiment after cold shock, Gravid day 2 adult cold-shocked worms were singled out immediately after the end of cold shock in a 12-well plates. Their progeny was assayed 3 days later and the P0 parent worm was transferred to a second well if it was alive 72h post cold shock, and its progeny was scored 3 days later.

Embryonic lethality assay and developmental delay

Gravid animals were allowed to lay eggs for two hours. A minimum of 100 embryos per condition were transferred onto a new plate, just outside of the bacterial lawn. The next day, embryos that did not hatch were scored as dead. At 65h post egg-laying synchronization at 20°C, the stage of each individual animal was determined. A developmental index was calculated by attributing a score from 1 to 6 to the successive stages L1, L2, L3, L4, young adult stage and gravid adult.

Lifespan

Lifespan assays were performed at either 20˚C or 25˚C as previously described (Morley and Morimoto 2004). Worms were synchronized by egg laying within 2 hours, as described above. A total of 50 hermaphrodites were cultured on each 6-cm NGM petri dish, seeded with 250 µLOP50. Animals were transferred to a fresh plate every 1 to 2 days until the cessation of progeny production and every 2 to 3 thereafter. Animals were scored every 2 to 3 days, and recorded as dead if they showed no spontaneous movement or response when probed on the nose. Animals dead from internal hatching (“bagging”), extruded intestine, and from desiccation on the side of the plate were censored. Statistical analysis was performed using GraphPad PRISM version 9.

Resistance to pathogenic bacteria

Experiments were performed at 25°C, according to (Kirienko et al. 2014; Scott et al. 2020). Fresh cultures of *Pseudomonas aeruginosa* PAO1 (<16h culture) were used to seed NGM plates. Plates were seeded with 50 µL bacterial culture by spreading on the totality of the NGM surface. Plates were left to dry for 48h before transferring the worms. Only fresh plates (no more than two days at room temperature) were used. For experiments involving N2 and MCL2, 40 µL of FUDR (5-Fluoro-2'deoxyuridine thymidylate synthase inhibitor) at 100mg/mL was pipetted onto each assay plate about 30 min-1h hour before transferring the worms on it, to prevent internal hatching, similar as in (Kirienko et al. 2014). Worms were fed OP50 bacteria until late L4 stage, when they were transferred on plates containing pathogenic bacteria. Not more than 40 worms were transferred onto each plate and worms were assayed every day.

Heat-shock

NGM plates were double sealed with parafilm and heat shocked in a water bath. Unless otherwise stated, heat shock was 30 minutes at 34°C. Worms were typically harvested immediately after heat shock.

Thermorecovery assay

The thermotolerance assay was performed as described previously (Labbadia and Morimoto 2015), except that heat-shock was 4h at 36°C. About 60-100 synchronized animals (late L4 stage) were picked onto a 6 cm NGM plate. Animals were then allowed to recover overnight at 20°C or 25°C. Animals were scored the next day at about 20h after the end of heat-shock. Animals were transferred onto a new plate and were counted as alive when they were either moving on the plate, or at least able to move their nose when poked with a pick.

Motility assay in *unc-54(e1301)* temperature sensitive mutants

Worms were raised at 15°C and transferred to 25°C at the L4 stage for experiments at the restrictive temperature. The motility was assayed 15h later. A circle of 1 cm diameter was drawn around the center of the lid of a 6 cm plate, which was placed under an NGM plate were OP50 bacteria were seeded at the periphery. Worms

were transferred at the center of the 1 cm diameter circle and their position was scored after 2 minutes, and classified in 3 zones: outside the circle, inside the circle or close to the center of the circle.

Cold recovery assay

At least 60 to 100 worms were transferred onto a fresh seeded NGM plate per condition. Plates were sealed with parafilm and buried upside down in a sterifoam box containing ice. The ice box was placed in a 4°C cold room for 4 hours. After the end of cold shock, plates were placed back in the incubator at the desired temperature for 20h, before scoring of survival.

Quantitative real-time PCR

To monitor steady-state mRNA levels, we handpicked a pool of about 50 animals per condition in 20 µL of RNAse free water. 500 µL of TRIzol was added and samples were processed as described in (He 2011). Reverse transcription was carried out using the Revert Aid First Strand synthesis kit from Thermo Scientific according to the manufacturer's instructions using oligo dT primers. The concentration of cDNA was monitored on a Nanodrop. Measurements of mRNA levels were obtained by qRT-PCR on a Lightcycler 480 (Roche). The amount of cDNA was quantified using the delta Ct quantification method, assuming 100% PCR efficiency for every couple of primers. For each couple The PCR efficiency was calculated for each couple of primers by running a standard curve on a dilution series. Validated couples of primers had a PCR efficiency between 90 and 113% with R2 > 0.98. Expression levels of steady-state mRNA were calculated using the ΔCt method.

Determination of housekeeping genes for qRT-PCR normalization

Primer sets (listed in Table S1) were designed to span exon-exon junctions (using NCBI Primer Blast software), and subsequently blasted against the *C. elegans* genome to test for off-target complementarity. It is crucial to verify the stability of the candidate housekeeping genes for normalization when assessing gene expression between different ploidies, to ensure that the expression of those genes relative to the others is not affected by the change of ploidy. Each target mRNA was normalized to

the average of the optimal number of the most stable housekeeping genes determined using the geNorm algorithm (Vandesompele et al. 2002), which establishes a hierarchy of stable genes from pairwise comparisons of expression levels across all conditions. For gene expression analysis performed at the L4 stage only, expression levels of target genes were normalized to the average of Y45F10D.4 and *act-1*. For gene expression analysis between L4 and day 2 adults, a second geNorm analysis was performed on genes expressed in the soma only (Knutson et al. 2017), to avoid potential artefacts coming from differences in the germline between diploids and tetraploids. Expression levels were normalized to the average of Y45F10D.4 and *lap-2* for qRT-PCR analysis at L4 and Day 2 adult stage.

Fluorescence microscopy and aggregates quantification

Animals were paralyzed in 3mM Levamisole diluted in M9, and mounted on a 2% agarose pad. Fluorescent images were taken on an epifluorescence Olympus IX81 microscope. At objective 10 X, unless otherwise stated. To quantify aggregates in worms carrying Q35:;YFP or Q44::YFP, the number of aggregates was counted for each individual worm on the original images, and normalized to the length of each worm (measured using FIJI/Image J), to account for body size increases in tetraploid lines. For visualization purpose, worms were straightened in some cases, using the FIJI/ImageJ macro Worm-align (Okkenhaug et al. 2020). Images of worms carrying the single copy transgene *hsp-16*p-lacO/UASp::LacI were taken on a Zeiss SP8 confocal microscope at objective 63X. Z-stacks were acquired using a step of 0.2 µm.

Monitoring of *hsp-16* DNA locus within the nucleus

The *hsp-16.2* DNA locus was visualized using the in vivo tracking system developed by (Rohner et al. 2013) using animals carrying the single copy transgene *gwSi3* [*hsp-16.2::wmCherry; 256x LacO; unc-119(+)]* together with the multicopy transgene *gwIs39[baf-1::gfp-LacI::let-858 3'UTR; vit-5::gfp]*, either in diploid (GW615) or in a tetraploid (MCL7) context. Gravid adults of each genetic background were dissected and embryos were mounted on a slide and immediately imaged on a confocal microscope. Z-stacks of early live embryos (not more than ~50 cell stage) were acquired on a confocal microscope. Heat-shock was performed next to the confocal microscope by warming the glass slide containing live embryos on a heating

block for 10 minutes at 34°C. Heat shocked embryos were immediately imaged at the end of heat shock. Measuring *hsp-16.2* DNA loci position in the nucleus was performed according to (Meister et al. 2010). Z-stacks containing images were visualized using the image analysis software Imaris (BITPLANE, Oxford Instruments). The *hsp-16.2* loci dots were selected and coloured differently from the diffuse nuclear GFP, based on GFP intensity thresholds (**Figure 2C**). The shortest distance to the nuclear envelope was measured for each *hsp-16.2* locus dot, together with the diameter of the nuclear plane in 2D images. The position of the foci was then classified in 3 zones of equal surface area, with zone 1 being the closest to the nuclear envelope (**Figure 2F**).

REFERENCES

Barker, Michael S., Nils Arrigo, Anthony E. Baniaga, Zheng Li, and Donald A. Levin. 2016. “On the Relative Abundance of Autopolyploids and Allopolyploids.” *New Phytologist* 210 (2): 391–98. https://doi.org/10.1111/nph.13698.

Birchler, James A., Nicole C. Riddle, Donald L. Auger, and Reiner A. Veitia. 2005. “Dosage Balance in Gene Regulation: Biological Implications.” *Trends in Genetics* 21 (4): 219–26. https://doi.org/10.1016/j.tig.2005.02.010.

Brenner, S. 1974. “The Genetics of Caenorhabditis Elegans.” *Genetics* 77 (1): 71–94.

Cadart, Clotilde, Julianne Bartz, Gillian Oaks, Martin Ziyuan Liu, and Rebecca Heald. 2023. “Polyploidy in Xenopus Lowers Metabolic Rate by Decreasing Total Cell Surface Area.” *Current Biology* 33 (9): 1744-1752.e7. https://doi.org/10.1016/j.cub.2023.03.071.

Chauve, Laetitia, Francesca Hodge, Sharlene Murdoch, Fatemah Masoudzadeh, Harry Jack Mann, Andrea Lopez-Clavijo, Hanneke Okkenhaug, et al. 2021. “Neuronal HSF-1 Coordinates the Propagation of Fat Desaturation across Tissues to Enable Adaptation to High Temperatures in C. Elegans.” *PLoS Biology* 19 (11). https://doi.org/10.1371/journal.pbio.3001431.

Clarke, Erlyana K., Katherine A. Rivera Gomez, Zaki Mustachi, Mikaela C. Murph, and Mara Schvarzstein. 2018. “Manipulation of Ploidy in Caenorhabditis Elegans.” *Journal of Visualized Experiments* 2018 (133): 1–11. https://doi.org/10.3791/57296.

David, Kyle. 2022. “Global Gradients in the Distribution of Animal Polyploids Kyle T. Davida,1 Edited.” *Proceedings of the National Academy of Sciences* 119 (48). https://doi.org/10.1073/pnas.

Deng, Benliang, Wenchao Du, Changlai Liu, Weiwei Sun, Shan Tian, and Hansong Dong. 2012. “Antioxidant Response to Drought, Cold and Nutrient Stress in Two Ploidy Levels of Tobacco Plants: Low Resource Requirement Confers Polytolerance in Polyploids?” *Plant Growth Regulation* 66 (1). https://doi.org/10.1007/s10725-011-9626-6.

Douglas, Peter M., Nathan A. Baird, Milos S. Simic, Sarah Uhlein, Mark A. McCormick, Suzanne C. Wolff, Brian K. Kennedy, and Andrew Dillin. 2015. “Heterotypic Signals from Neural HSF-1 Separate Thermotolerance from Longevity.” *Cell Reports* 12 (7): 1196–1204. https://doi.org/10.1016/j.celrep.2015.07.026.

Doyle, Jeff J., and Jeremy E. Coate. 2019. “Polyploidy, the Nucleotype, and Novelty: The Impact of Genome Doubling on the Biology of the Cell.” *International Journal of Plant Sciences* 180 (1): 1–52. https://doi.org/10.1086/700636.

Flemming, Anthony J., Zai Zhong Shen, Ana Cunha, Scott W. Emmons, and Armand M. Leroi. 2000. “Somatic Polyploidization and Cellular Proliferation Drive Body Size Evolution in Nematodes.” *Proceedings of the National Academy of Sciences of the United States of America* 97 (10): 5285–90. https://doi.org/10.1073/pnas.97.10.5285.

Gulyas, Leah, and Jennifer R. Powell. 2022. “Cold Shock Induces a Terminal Investment Reproductive Response in C. Elegans.” *Scientific Reports* 12 (1): 1–14. https://doi.org/10.1038/s41598-022-05340-6.

Gumienny, Tina L., and Cathy Savage-Dunn. 2013. “TGF-β Signaling in C. Elegans.” *WormBook : The Online Review of C. Elegans Biology*, 1–34. https://doi.org/10.1895/wormbook.1.22.2.

Harari, Yaniv, Yoav Ram, Nimrod Rappoport, Lilach Hadany, and Martin Kupiec. 2018. “Spontaneous Changes in Ploidy Are Common in Yeast.” *Current Biology* 28 (6): 825-835.e4. https://doi.org/10.1016/j.cub.2018.01.062.

He, Fanglian. 2011. “Total RNA Extraction from C. Elegans.” *BIO-PROTOCOL* 1 (6). https://doi.org/10.21769/bioprotoc.47.

Jatllon, Olivier, Jean Marc Aury, Frédéric Brunet, Jean Louis Petit, Nicole Stange-Thomann, Evan Maucell, Laurence Bouneau, et al. 2004. “Genome Duplication in the Teleost Fish Tetraodon Nigroviridis Reveals the Early Vertebrate Proto-Karyotype.” *Nature* 431 (7011). https://doi.org/10.1038/nature03025.

Jiang, Wei, Yuehua Wei, Yong Long, Arthur Owen, Bingying Wang, Xuebing Wu, Shuo Luo, Yongjun Dang, and Dengke K. Ma. 2018. “A Genetic Program Mediates Cold-Warming Response and Promotes Stress-Induced Phenoptosis in C. Elegans.” *ELife* 7. https://doi.org/10.7554/eLife.35037.

Jiang, Yulan, Shiliang Liu, Ju Hu, Guangti He, Yingqi Liu, Xi Chen, Ting Lei, et al. 2020. “Polyploidization of Plumbago Auriculata Lam. in Vitro and Its Characterization Including Cold Tolerance.” *Plant Cell, Tissue and Organ Culture* 140 (2). https://doi.org/10.1007/s11240-019-01729-w.

Kemp, Benedict J., Diane L. Church, Julia Hatzold, Barbara Conradt, and Eric J. Lambie. 2009. “Gem-1 Encodes an SLC16 Monocarboxylate Transporter-Related Protein That Functions in Parallel to the Gon-2 TRPM Channel during Gonad Development in Caenorhabditis Elegans.” *Genetics* 181 (2). https://doi.org/10.1534/genetics.108.094870.

Kirienko, Natalia V., Brent O. Cezairliyan, Frederick M. Ausubel, and Jennifer R. Powell. 2014. “Pseudomonas Aeruginosa PA14 Pathogenesis in Caenorhabditis Elegans.” *Methods in Molecular Biology* 1149. https://doi.org/10.1007/978-1-4939-0473-0_50.

Knutson, Andrew Kekūpa’a, Thea Egelhofer, Andreas Rechtsteiner, and Susan Strome. 2017. “Germ Granules Prevent Accumulation of Somatic Transcripts in the Adult Caenorhabditis Elegans Germline.” *Genetics* 206 (1): 163–78. https://doi.org/10.1534/genetics.116.198549.

Labbadia, Johnathan, and Richard I. Morimoto. 2015. “Repression of the Heat Shock Response Is a Programmed Event at the Onset of Reproduction.” *Molecular Cell* 59 (4). https://doi.org/10.1016/j.molcel.2015.06.027.

Lee, Seung Jae, and Cynthia Kenyon. 2009. “Regulation of the Longevity Response to Temperature by Thermosensory Neurons in Caenorhabditis Elegans.” *Current Biology* 19 (9): 715–22. https://doi.org/10.1016/j.cub.2009.03.041.

Li, Tian Neng, Yi Ju Wu, Hung Wen Tsai, Cheng Pu Sun, Yi Hsuan Wu, Hui Lin Wu,

Yi Ning Pei, et al. 2018. “Intrahepatic Hepatitis B Virus Large Surface Antigen Induces Hepatocyte Hyperploidy via Failure of Cytokinesis.” *Journal of Pathology* 245 (4). https://doi.org/10.1002/path.5102.

Lin, Yu Hsuan, Shuyuan Zhang, Min Zhu, Tianshi Lu, Kenian Chen, Zhuoyu Wen, Shidan Wang, et al. 2020. “Mice With Increased Numbers of Polyploid Hepatocytes Maintain Regenerative Capacity But Develop Fewer Hepatocellular Carcinomas Following Chronic Liver Injury.” *Gastroenterology* 158 (6). https://doi.org/10.1053/j.gastro.2020.01.026.

Lindquist, Susan. 1986. “THE HEAT-SHOCK RESPONSE.” www.annualreviews.org.

Losick, Vicki P., Donald T. Fox, and Allan C. Spradling. 2013. “Polyploidization and Cell Fusion Contribute to Wound Healing in the Adult Drosophila Epithelium.” *Current Biology* 23 (22). https://doi.org/10.1016/j.cub.2013.09.029.

Lozano, Encarnación, Alberto G. Sáez, Anthony J. Flemming, Ana Cunha, and Armand M. Leroi. 2006. “Regulation of Growth by Ploidy in Caenorhabditis Elegans.” *Current Biology* 16 (5): 493–98. https://doi.org/10.1016/j.cub.2006.01.048.

Lu, Yi Jin, Krishna B.S. Swamy, and Jun Yi Leu. 2016. “Experimental Evolution Reveals Interplay between Sch9 and Polyploid Stability in Yeast.” *PLoS Genetics* 12 (11): 1–26. https://doi.org/10.1371/journal.pgen.1006409.

Mable, B. K., M. A. Alexandrou, and M. I. Taylor. 2011. “Genome Duplication in Amphibians and Fish: An Extended Synthesis.” *Journal of Zoology* 284 (3): 151–82. https://doi.org/10.1111/j.1469-7998.2011.00829.x.

Madl, J. E., and R. K. Herman. 1979. “Polyploids and Sex Determination in Caenorhabditis Elegans.” *Genetics* 93 (2): 393–402. https://doi.org/10.1093/genetics/93.2.393.

Makino, Takashi, and Aoife McLysaght. 2010. “Ohnologs in the Human Genome Are Dosage Balanced and Frequently Associated with Disease.” *Proceedings of the National Academy of Sciences of the United States of America* 107 (20): 9270–74. https://doi.org/10.1073/pnas.0914697107.

Mehlferber, Elijah C, Michael J Song, Julianne Naomi Pelaez, Johan Jaenisch, E Jeremy, Britt Koskella, and Carl J Rothfels. 2021. “Induction of Autotetrapolyploidy and Microbiome Associations Mediate Differential Responses Responses to Pathogens.” *BioRxiv*, 1–23.

Meister, Peter, Lutz R. Gehlen, Elisa Varela, Véronique Kalck, and Susan M. Gasser. 2010. *Visualizing Yeast Chromosomes and Nuclear Architecture*. *Methods in Enzymology*. 2nd ed. Vol. 470. Elsevier Inc. https://doi.org/10.1016/S0076-6879(10)70021-5.

Misare, Kelly R, Elizabeth A Ampolini, Hyland C Gonzalez, Kaitlan A Sullivan, Xin Li, Camille Miller, Bintou Sosseh, et al. 2023. “The Consequences of Tetraploidy on Caenorhabditis Elegans Physiology and Sensitivity to Chemotherapeutics.”

Mok, Darren Z.L., Paul W. Sternberg, and Takao Inoue. 2015. “Morphologically Defined Sub-Stages of C. Elegans Vulval Development in the Fourth Larval Stage.” *BMC Developmental Biology* 15 (1). https://doi.org/10.1186/s12861-015-

0076-7.

Morley, James F., Heather R. Brignull, Jill J. Weyers, and Richard I. Morimoto. 2002. "The Threshold for Polyglutamine-Expansion Protein Aggregation and Cellular Toxicity Is Dynamic and Influenced by Aging in Caenorhabditis Elegans." *Proceedings of the National Academy of Sciences of the United States of America* 99 (16): 10417–22. https://doi.org/10.1073/pnas.152161099.

Morley, James F., and Richard I. Morimoto. 2004. "Regulation of Longevity in Caenorhabditis Elegans by Heat Shock Factor and Molecular Chaperones." *Molecular Biology of the Cell*. https://doi.org/10.1091/mbc.E03-07-0532.

Nakatani, Yoichiro, Prashant Shingate, Vydianathan Ravi, Nisha E. Pillai, Aravind Prasad, Aoife McLysaght, and Byrappa Venkatesh. 2021. "Reconstruction of Proto-Vertebrate, Proto-Cyclostome and Proto-Gnathostome Genomes Provides New Insights into Early Vertebrate Evolution." *Nature Communications* 12 (1): 1–14. https://doi.org/10.1038/s41467-021-24573-z.

Nakatani, Yoichiro, Hiroyuki Takeda, Yuji Kohara, and Shinichi Morishita. 2007. "Reconstruction of the Vertebrate Ancestral Genome Reveals Dynamic Genome Reorganization in Early Vertebrates." *Genome Research* 17 (9): 1254–65. https://doi.org/10.1101/gr.6316407.

Nigon, V. 1949. "Effets de La Polyploïdie Chez Un Nématode Libre." *Comptes Rendus Hebdomadaires Des Séances de l'Académie* 228 (13).

Novikova, Polina Yu, Ian G. Brennan, William Booker, Michael Mahony, Paul Doughty, Alan R. Lemmon, Emily Moriarty Lemmon, et al. 2020. "Polyploidy Breaks Speciation Barriers in Australian Burrowing Frogs Neobatrachus." *PLoS Genetics* 16 (5): 1–24. https://doi.org/10.1371/journal.pgen.1008769.

Ohta, Akane, Tomoyo Ujisawa, Satoru Sonoda, and Atsushi Kuhara. 2014. "Light and Pheromone-Sensing Neurons Regulates Cold Habituation through Insulin Signalling in Caenorhabditis Elegans." *Nature Communications* 5 (July). https://doi.org/10.1038/ncomms5412.

Okahata, Misaki, Haruka Motomura, Akane Ohta, and Atsushi Kuhara. 2022. "Molecular Physiology Regulating Cold Tolerance and Acclimation of Caenorhabditis Elegans." *Proceedings of the Japan Academy Series B: Physical and Biological Sciences* 98 (3): 126–39. https://doi.org/10.2183/pjab.98.009.

Okkenhaug, Hanneke, Laetitia Chauve, Fatemeh Masoudzadeh, Lars Okkenhaug, and Olivia Casanueva. 2020. "Worm-Align and Worm_CP, Two Open-Source Pipelines for Straightening and Quantification of Fluorescence Image Data Obtained from Caenorhabditis Elegans." *Journal of Visualized Experiments* 2020 (159): 1–13. https://doi.org/10.3791/61136.

Oswald, Benjamin P., and Scott L. Nuismer. 2007. "Neopolyploidy and Pathogen Resistance." *Proceedings of the Royal Society B: Biological Sciences* 274 (1624): 2393–97. https://doi.org/10.1098/rspb.2007.0692.

Otto, S. P., and J. Whitton. 2000. "Polyploid Incidence and Evolution." *Annual Review of Genetics*. https://doi.org/10.1146/annurev.genet.34.1.401.

Peer, Yves Van de, Tia Lynn Ashman, Pamela S. Soltis, and Douglas E. Soltis. 2021. “Polyploidy: An Evolutionary and Ecological Force in Stressful Times.” *The Plant Cell* 33 (1): 11–26. https://doi.org/10.1093/plcell/koaa015.

Peer, Yves Van De, Eshchar Mizrachi, and Kathleen Marchal. 2017. “The Evolutionary Significance of Polyploidy.” *Nature Reviews Genetics* 18 (7): 411–24. https://doi.org/10.1038/nrg.2017.26.

Pozo, Juan C. Del, and Elena Ramirez-Parra. 2014. “Deciphering the Molecular Bases for Drought Tolerance in Arabidopsis Autotetraploids.” *Plant, Cell and Environment* 37 (12): 2722–37. https://doi.org/10.1111/pce.12344.

Rice, Anna, Petr Šmarda, Maria Novosolov, Michal Drori, Lior Glick, Niv Sabath, Shai Meiri, Jonathan Belmaker, and Itay Mayrose. 2019. “The Global Biogeography of Polyploid Plants.” *Nature Ecology and Evolution* 3 (2). https://doi.org/10.1038/s41559-018-0787-9.

Roelens, Baptiste, Mara Schvarzstein, and Anne M. Villeneuve. 2015. “Manipulation of Karyotype in Caenorhabditis Elegans Reveals Multiple Inputs Driving Pairwise Chromosome Synapsis during Meiosis.” *Genetics* 201 (4): 1363–79. https://doi.org/10.1534/genetics.115.182279.

Rohner, Sabine, Veronique Kalck, Xuefei Wang, Kohta Ikegami, Jason D. Lieb, Susan M. Gasser, and Peter Meister. 2013. “Promoter-and RNA Polymerase II-Dependent Hsp-16 Gene Association with Nuclear Pores in Caenorhabditis Elegans.” *Journal of Cell Biology* 200 (5): 589–604. https://doi.org/10.1083/jcb.201207024.

Ryan Gregory, T., and Barbara K. Mable. 2004. “Polyploidy in Animals.” In *The Evolution of the Genome*. https://doi.org/10.1016/B978-012301463-4/50010-3.

Saei, A., K. Hoeata, A. Krebs, P. Sutton, J. Herrick, M. Wood, and L. Gea. 2018. “The Status of Pseudomonas Syringae Pv. Actinidiae (Psa) in the New Zealand Kiwifruit Breeding Programme in Relation to Ploidy Level.” In *Acta Horticulturae*. Vol. 1218. https://doi.org/10.17660/ActaHortic.2018.1218.40.

Schindelin, Johannes, Ignacio Arganda-Carreras, Erwin Frise, Verena Kaynig, Mark Longair, Tobias Pietzsch, Stephan Preibisch, et al. 2012. “Fiji: An Open-Source Platform for Biological-Image Analysis.” *Nature Methods* 9 (7): 676–82. https://doi.org/10.1038/nmeth.2019.

Schvarzstein, Mara, Fatema Alam, Muhammad Toure, and Judith L Yanowitz. 2023. “An Emerging Animal Model for Querying the Role of Whole Ge- Nome Duplication in Development , Evolution , and Disease Polyploidization,” no. April: 1–24. https://doi.org/10.20944/preprints202304.0989.v1.

Scott, Euan, Lindy Holden-Dye, Vincent O’Connor, and Matthew E. Wand. 2020. “Intra Strain Variation of the Effects of Gram-Negative ESKAPE Pathogens on Intestinal Colonization, Host Viability, and Host Response in the Model Organism Caenorhabditis Elegans.” *Frontiers in Microbiology* 10. https://doi.org/10.3389/fmicb.2019.03113.

Selmecki, Anna M., Yosef E. Maruvka, Phillip A. Richmond, Marie Guillet, Noam Shoresh, Amber L. Sorenson, Subhajyoti De, et al. 2015. “Polyploidy Can Drive Rapid Adaptation in Yeast.” *Nature* 519 (7543): 349–51.

https://doi.org/10.1038/nature14187.

Simakov, Oleg, Ferdinand Marlétaz, Jia Xing Yue, Brendan O'Connell, Jerry Jenkins, Alexander Brandt, Robert Calef, et al. 2020. "Deeply Conserved Synteny Resolves Early Events in Vertebrate Evolution." *Nature Ecology and Evolution* 4 (6): 820–30. https://doi.org/10.1038/s41559-020-1156-z.

Sladky, Valentina C., Felix Eichin, Thomas Reiberger, and Andreas Villunger. 2021. "Polyploidy Control in Hepatic Health and Disease." *Journal of Hepatology*. https://doi.org/10.1016/j.jhep.2021.06.030.

Syngelaki, Eleni, Claudia Paetzold, and Elvira Hörandl. 2021. "Gene Expression Profiles Suggest a Better Cold Acclimation of Polyploids in the Alpine Species Ranunculus Kuepferi (Ranunculaceae)." *Genes* 12 (11). https://doi.org/10.3390/genes12111818.

Vandesompele, Jo, Katleen De Preter, ilip Pattyn, Bruce Poppe, Nadine Van Roy, Anne De Paepe, and rank Speleman. 2002. "Accurate Normalization of Real-Time Quantitative RT-PCR Data by Geometric Averaging of Multiple Internal Control Genes." http://genomebiology.com/2002/3/7/research/0034.1Correspondence:.rankSpeleman.

Wang, Changnan, Yong Long, Bingying Wang, Chao Zhang, and Dengke K. Ma. 2023. "GPCR Signaling Regulates Severe Stress-Induced Organismic Death in Caenorhabditis Elegans." *Aging Cell* 22 (1): 1–12. https://doi.org/10.1111/acel.13735.

Wang, Weining, Yanhong He, Zhe Cao, and Zhanao Deng. 2018. "Induction of Tetraploids in Impatiens (Impatiens Walleriana) and Characterization of Their Changes in Morphology and Resistance to Downy Mildew." *HortScience* 53 (7): 925–31. https://doi.org/10.21273/HORTSCI13093-18.

Was, Halina, Agata Borkowska, Aleksandra Olszewska, Aleksandra Klemba, Marta Marciniak, Agnieszka Synowiec, and Claudine Kieda. 2022. "Polyploidy Formation in Cancer Cells: How a Trojan Horse Is Born." *Seminars in Cancer Biology* 81 (October 2020): 24–36. https://doi.org/10.1016/j.semcancer.2021.03.003.

Wolfe, Kenneth H. 2015. "Origin of the Yeast Whole-Genome Duplication." *PLoS Biology* 13 (8): 1–7. https://doi.org/10.1371/journal.pbio.1002221.

Zhou, Li, and Jianfang Gui. 2017. "Natural and Artificial Polyploids in Aquaculture." *Aquaculture and Fisheries*. https://doi.org/10.1016/j.aaf.2017.04.003.

FIGURES LEGENDS

Figure 1- Synthetic autotetraploid *C. elegans* animals exhibit decreased fitness under regular conditions. (**A**) Images of most mature unfertilized oocyte nuclei, stained with DAPI, before the first meiotic division of diploid N2 (WT) worms (top) showing 6 bivalent chromosomes, and derived MCL2 (4n) teraploid animals, showing 12 bivalents. Maximum intensity projection, Confocal, objective 63X. Scale bar is 8µm. (**B**) MCL2 (4n) tetraploid animals are developmentally delayed. Developmental stage at 65h post egg-laying synchronisation at 20°C. Stages: L1,L2,L3,L4, young adult (YA), and gravid adult (GA) are numbered from 1 to 6 respectively. (**C**) Tetraploid MCL2 (4n) are delayed compared to diploid animals. A developmental index was calculated by multiplying frequencies by numbered developmental stage at 65h post synchronisation at 20°C. P-value N2 vs MCL2 =0.0049.The average tetraploid population is estimated to be 8-10h delayed compared to its diploid counterpart. Three biological replicates. (**D**) Derived tetraploids MCL1 (4n#1) and MCL2 (4n#2) exhibit higher rates of embryonic lethality at 20°C than diploid WT N2 (2n). Three biological replicates. (**E**) Derived tetraploids MCL1 (4n#1) and MCL2 (4n#2) exhibit decreased fertlity compared to WT N2 (2n) animals. Averagel number of progeny per worm: N2: 231.5, MCL1: 61.46, MCL2: 65.97. (**F**) Images of of diploid N2 and tetraploid MCL2 animals at both L4 (top) and Day 2 adult stage (L4 + 24h, bottom). Scale bar is 100 µm. (**G-H**) Body volume measurments at 20°C of diploid N2 (2n), derived tetraploid MCL2 (4n) and *dl-1(nk3)* (2n) loss of function mutants during development (G) or during adulthood (H). (G) Number of animals measured per biological replicate: N2:16, MCL2:14, NU3:15. (**H**) L4 animals were selected at the late larval substages, as L4.9 stage (Mok, Sternberg, and Inoue 2015), ~2h before the young adult stage. (H) Number of animals measured in 3 to 5 independent biological replicates: N2:n=330, MCL2: n=261, NU3: n=261. (**I**) Ratios of body volume measurments at day 2 adult stage compared to L4 stage for N2 (2n), MCL2 (4n) and *dbl-1(nk3)* (2n) mutant. Average ratio increase between L4 and day 2 adults: N2: 3 to 5.57 fold, MCL2: 1.3 to 2.83 fold, NU3: 2.03 to 2.8 fold. One-way Anova. (**J**) Lifespan at 20°C of WT N2 (2n) and derived tetraploid lines MCL1 (4n#1) and MCL2 (4n#2).Number of animals assayed: 148-150 per genotype. p-value N2 (2n) vs MCL1 (4n #1): p-value<0.0001 (****), N2 (2n) vs MCL2 (4n #2): p-value<0.0001 (****). (**K**) Lifespan at 25°C of WT N2 (2n) and derived tetraploid lines MCL1 (4n#1) and MCL2 (4n#2). Number of animals assayed: 148-150 per genotype p-value N2 (2n) vs MCL1 (4n #1) = 0.8008 (ns), p-value N2 (2n) vs MCL2 (4n #2) = 0.0869 (ns).

Figure 2- Synthetic autotetraploid *C. elegans* display improved resistance to heat stress but similar resistance to pathogenic bacteria. (**A**) Survival of N2 (2n) and derived tetraploid MCL2 (4n #2) animals exposed to 4h heat stress at 35°C, followed by 20h recovery at 20°C. Two-way ANOVA: ploidy effect: p=0.0070 (**), temperature effect: p=0.3730 (ns), ploidy x temperature: p=0.6662 (ns). Independent biological replicates are coloured. (**B**) Kinetics of inducible molecular chaperones *hsp-16.1* (top) and *hsp-16.2* (bottom) mRNA induction following heat shock is altered. mRNA were monitored in WT N2 (2n) and derived tetraploid MCL1 (4n #1) and MCL2 (4n #2) animals.(**C**) Micrographs of early embryonic nuclei (~50 cell stage) from GW615 (2n) or derived tetraploid MCL7 (4n) animals carrying both transgenes *baf-1*p::GFP-LacI and *hsp-16.2p*-LacO (Rohner et al. 2013). Nuclei were images at 63X obj. on a confocal and visualised using Imaris software, with nuclear fluorescence from *baf-1p::*GFP-LacI in blue and *hsp-16.2*p-LacO DNA loci in pink.(**D-E**) Density plots representing the distance to the nuclear envelop (dNE) of *hsp-16.2p*-LacO loci in the absence of heat shock (HS) (D) or 10-20 minutes following a 10 minutes HS at 34°C (E) in GW615 (2n) or derived tetraploid MCL7 (4n). Data in (D): GW615: 49 nuclei (96 dots), MCL7: 20 nuclei (54 dots). Unpaired t-test GW615 vs MCL7: p-value=0.5715. Data in (E): GW615: 47 nuclei (88 dots), MCL7: 38 nuclei (119 dots). Unpaired t-test GW615 vs MCL7: p-value= 0.0204. Dashed lines in D and E represent the median. (**F**) Schematic representation of *hsp-16.2p*-LacO DNA locus intranuclear position measurements according to the method developped in (Rohner et al. 2013; Meister et al. 2010). For each dot, the distance to the nuclear envelop (dNE) was measured as well as the diameter of the nuclear plane. (**G-H**) Classification of *hsp-16.2p*-LacO genomic DNA loci positions in 3 zones of equal surfaces within the nuclear plane, as defined in (Rohner et al. 2013), in the absence (G) of HS, or following a short HS of 10 minutes at 34°C (H), for diploid GW615 and tetraploid MCL7 nuclei. (G): Chi-square GW615 vs MCL7: p-value = 0.8638 (ns). (H): Chi-square GW615 vs MCL7: p-value=0.0019 (**). (**I**) Survival of WT diploid N2 (2n) and derived tetraploid MCL2 (4n #2) animals raised on pathogenic *Pseudomonas aeruginosa* PAO1 bacteria from L4 stage on. Animals were grown on plates containing DNA synthesis inhibitor FuDR (5-Fluorodeoxyribouridine) to prevent egg-hatching and bagging, common upon PAO1 exposure. Experiment performed at 25°C. p-value N2 (2n) vs MCL2 (4n) = 0.7546 (ns). (**J**) Survival of gonadless WT diploid EJ1171 (2n) *gon-2(q388); gem-1(bc364)* temperature sensitive (ts) mutants and derived gonadless tetraploid MCL22 (4n) animals raised on pathogenic *Pseudomonas aeruginosa* PAO1 bacteria from L4 stage on. Experiment performed at 25°C. p-value EJ1171 (2n) vs MCL22 (4n) = 0.9263 (ns).

Figure 3- Synthetic autotetraploid *C. elegans* escape cold induced death at the adult stage and produce more progeny than diploids. (**A**) Schematic overview of cold recovery assay. Plates containing animals raised at 20°C were placed in ice for 4h, followed by a 20h recovery period at 20°C. (**B**) Survival upon cold recovery of diploid N2 (2n) and derived tetraploid MCL2 (4m #2) at L4 or Day 2 adult stage (D2). One way Anova. L4: p-value N2 vs MCL2 = 0.8122. D2: p-value N2 vs MCL2= 0.0047. (**C**) Survival upon cold recovery at Day 2 adult stage of diploid N2 (2n) and derived tetraploid MCL2 (4m #2) grown on plates containing DNA synthesis inhibitor FuDR (5-Fluorodeoxyribouridine) to prevent egg-hatching and bagging. Paired t-test: p-value N2 vs MCL2= 0.0045. (**D**) Survival upon cold recovery of gonadless diploid EJ1171 (2n) *gon-2(q388); gem-1(bc364)* ts mutants and derived gonadless tetraploid MCL22 (4n) at L4 or Day 2 adult stage (D2). One way Anova. L4: p-value EJ1171 vs MCL22 = 0.9843. D2: p-value EJ1171 vs MCL22= 0.5390. (**E**) Survival upon cold recovery of diploid N2 (2n) and derived tetraploid MCL2 (4m #2) at L4 or Day 2 adult stage. Animals were either raised at 15°C (cold acclimatation) or at 25°C. One way Anova. 15°C: p-value N2 vs MCL2 at L4 = 0.9850, p-value N2 vs MCL2 at day 2 = 0.7363.. 25°C: p-value N2 vs MCL2 at L4 = 0.5308, p-value N2 vs MCL2 at D2 = 0.0047. (**F**) Average number of progeny per P0 worms of diploid N2 (2n) or derived tetraploid MCL2 (4n #2) exposed to cold recovery at D2 adult stage. Paired t-test: p-value N2 vs MCL2= 0.0161. In all panels, colours indicate independent biological replicates.

Figure 4- Progeny of cold-shocked autotetraploids animals is of similar quality than the progeny of cold-shock diploid animals. (**A**) Schematic overview of different time points after cold-shock (CS) and recovery at which F1 progeny of diploid and tetraploid cold shock P0 was assayed. Around 16h post cold shock, the majority of P0 diploid CS was dead. (**B**) Percentage of embryonic lethality in the progeny of diploid N2 (2n, grey) and derived tetraploid MCL2 (4n #2 blue) in the absence of CS (dashed lines) or following CS (full lines), at different time points after CS. Two way Anova across all time points. Without CS: p-value ploidy effect: 0.0798 (ns), p-value time=0.7405 (ns), p-value ploidy x time: 0.8645 (ns). After CS: p-value ploidy effect: 0.0504 (ns), p-value time= 0.2714 (ns), p-value ploidy x time= 0.6431 (ns). (**C**) Survival upon cold recovery of F1 progeny of cold-shocked P0 diploid N2 (2n) or derived tetraploid MCL2 (4n #2) animals at the L4 stage. F1 progeny were asseyed at different time points after CS of P0 animals. Mixed effect analysis: p-value N2 vs MCL2= 0.4489 (ns). Pairwise adjusted p-values (Sidak's multiple comparisons test) are indicated on the graph. (**D-G**) Developmental index of the F1 progeny of CS P0 diploid N2 (2n) or derived tetraploid MCL2 (4n) animals. (F1 progeny was collected right after CS of P0 (D-E) or at 3h post CS of P0s (F-G). As tetraploid MCL2 are developmentally delayed compared to diploid N2 animals, the developmental index of the F1 progeny cold-shocked of diploid and tetraploid was compared to the progeny of non

cold-shocked diploid and tetraploid animals respectively. (D-F) A developmental index was calculated by multiplying ferquencies by numbered developmental stage at 65h post synchronisation at 20°C. (D) Two-way Anova: p-value poidy effect=0.0191(*), p-value CS status in P0= 0.0067(**), p-value interaction ploidy x CS status in P0= 0.1114 (ns). Pairwise adjusted p-values from Sidak's multiple comparison tests are indicated on the graph. (F) Two-way Anova: p-value poidy effect=0.0507(ns), p-value CS status in P0= 0.0741(ns), p-value interaction ploidy x CS status in P0= 0.0871(ns). Pairwise adjusted p-values from Sidak's multiple comparison tests are indicated on the graph. (E-G) Ratio of developmental index of the progeny of cold-shocked P0s over the developmental index of the progeny of non cold-shcked P0s. P-values from paired t-tests are indicated on the graphs in E and G. In all panels, colours indicate independent biological replicates.

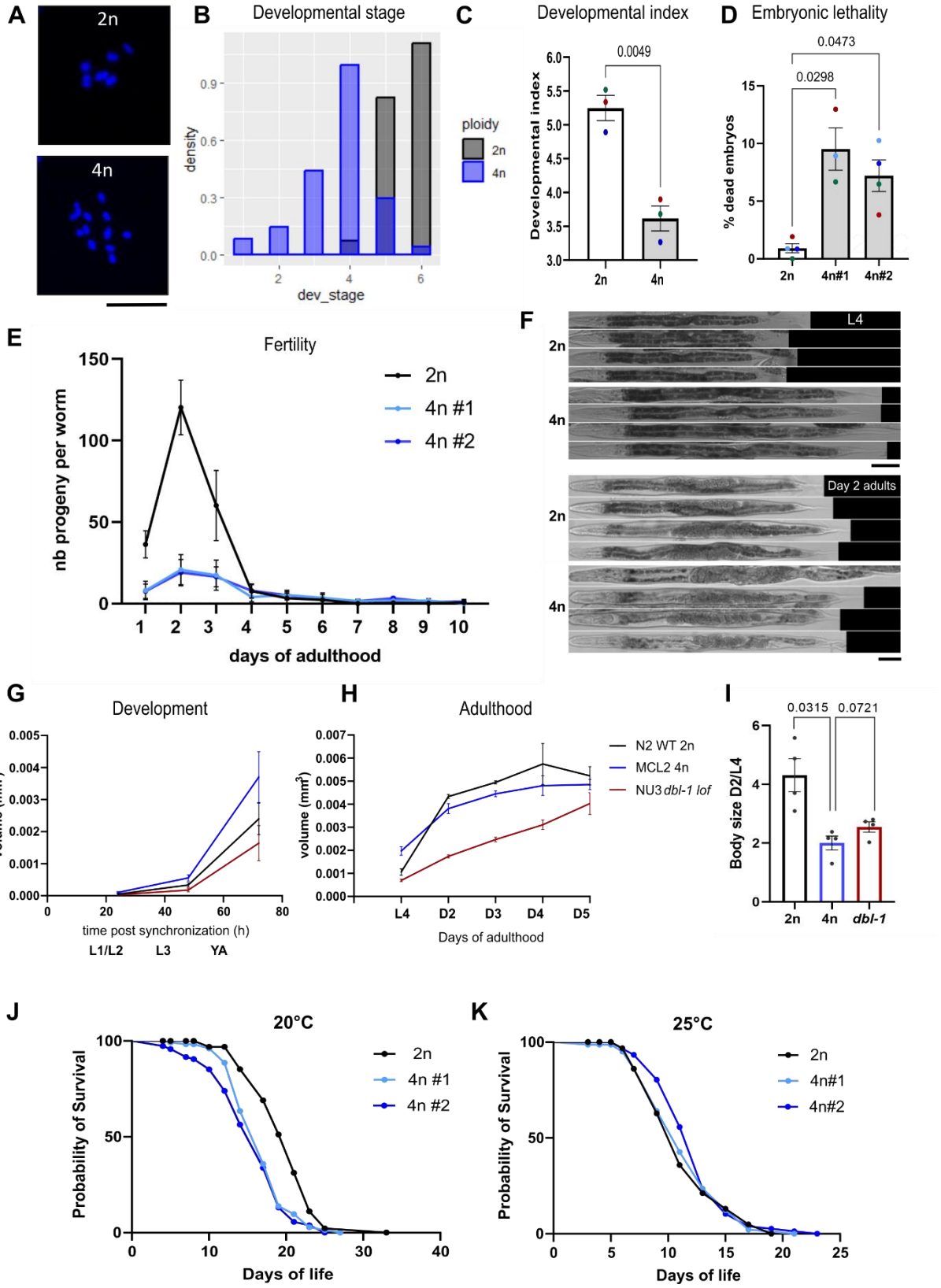
A
2n
4n
B
Developmental stage
density
dev_stage
ploidy
2n
4n
C
Developmental index
Developmental index
0.0049
2n
4n
D
Embryonic lethality
% dead embryos
0.0473
0.0298
2n
4n#1
4n#2
E
Fertility
nb progeny per worm
days of adulthood
2n
4n #1
4n #2
F
L4
Day 2 adults
2n
4n
G
Development
volume (mm³)
time post synchronization (h)
L1/L2
L3
YA
H
Adulthood
volume (mm³)
Days of adulthood
L4
D2
D3
D4
D5
N2 WT 2n
MCL2 4n
NU3 dbl-1 lof
I
Body size D2/L4
0.0315
0.0721
2n
4n
dbl-1
J
20°C
Probability of Survival
Days of life
2n
4n #1
4n #2
K
25°C
Probability of Survival
Days of life
2n
4n#1
4n#2

Figure 1.

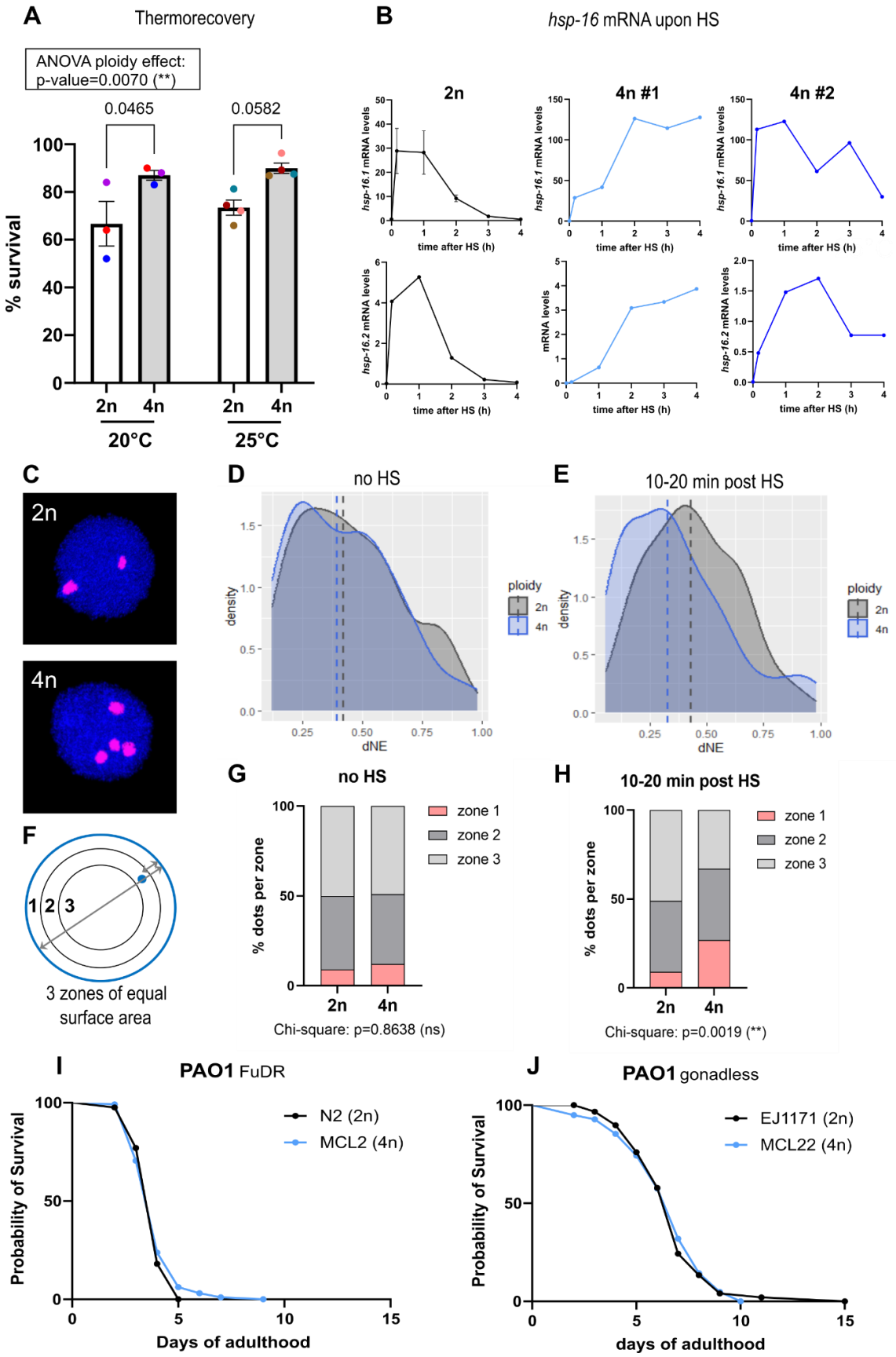
A
Thermorecovery
ANOVA ploidy effect:
p-value=0.0070 (**)
0.0465
0.0582
% survival
2n
4n
20°C
25°C
B
hsp-16 mRNA upon HS
2n
4n #1
4n #2
hsp-16.1 mRNA levels
hsp-16.2 mRNA levels
mRNA levels
time after HS (h)
C
2n
4n
D
no HS
density
dNE
ploidy
E
10-20 min post HS
F
1 2 3
3 zones of equal surface area
G
no HS
% dots per zone
zone 1
zone 2
zone 3
Chi-square: p=0.8638 (ns)
H
10-20 min post HS
Chi-square: p=0.0019 (**)
I
PAO1 FuDR
Probability of Survival
N2 (2n)
MCL2 (4n)
Days of adulthood
J
PAO1 gonadless
EJ1171 (2n)
MCL22 (4n)
days of adulthood

Figure 2.

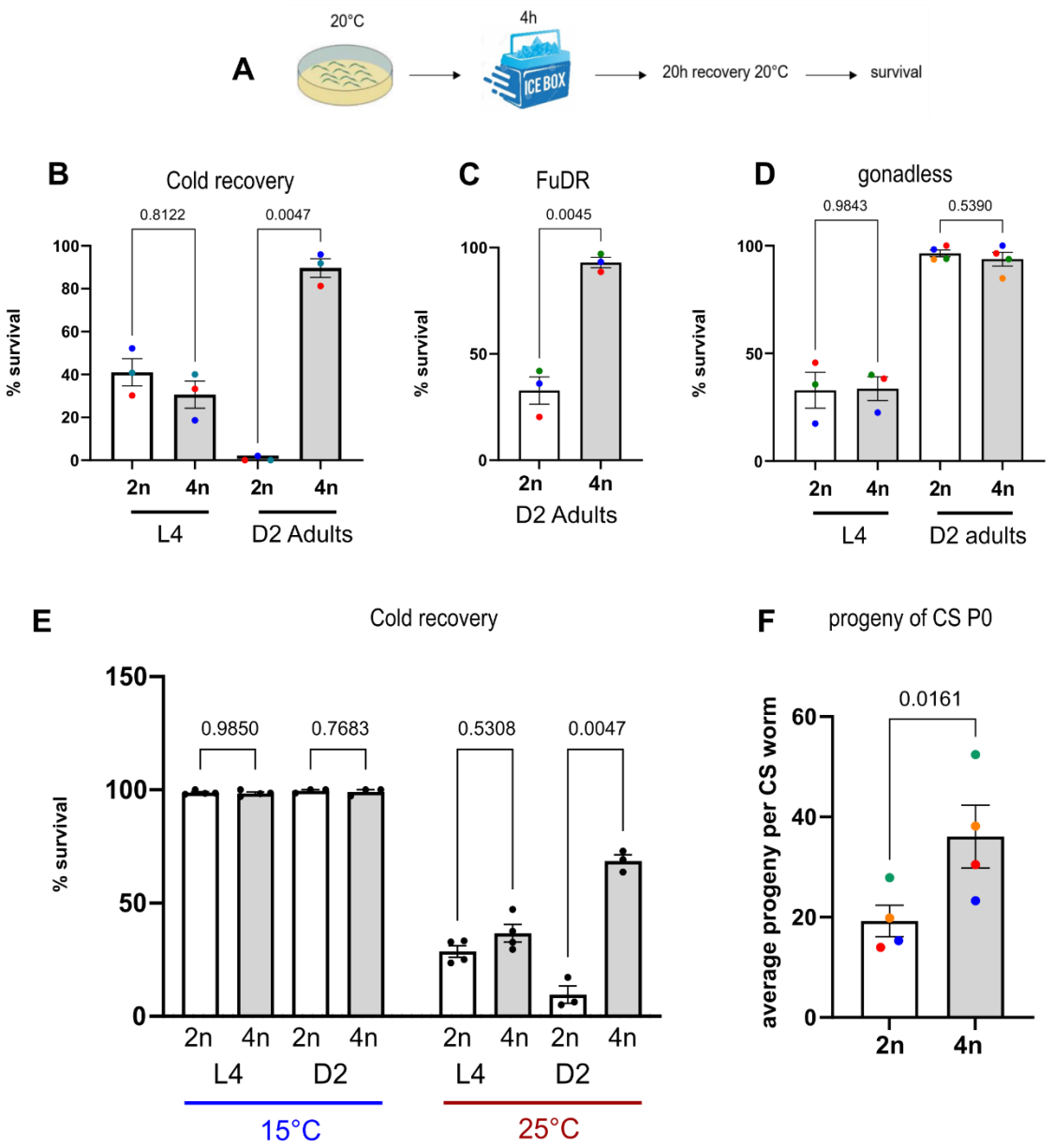
A
20°C
4h
ICE BOX
20h recovery 20°C
survival
B
Cold recovery
0.8122
0.0047
% survival
2n
4n
2n
4n
L4
D2 Adults
C
FuDR
0.0045
% survival
2n
4n
D2 Adults
D
gonadless
0.9843
0.5390
% survival
2n
4n
2n
4n
L4
D2 adults
E
Cold recovery
% survival
0.9850
0.7683
0.5308
0.0047
2n
4n
2n
4n
2n
4n
2n
4n
L4
D2
L4
D2
15°C
25°C
F
progeny of CS P0
average progeny per CS worm
0.0161
2n
4n

Figure 3.

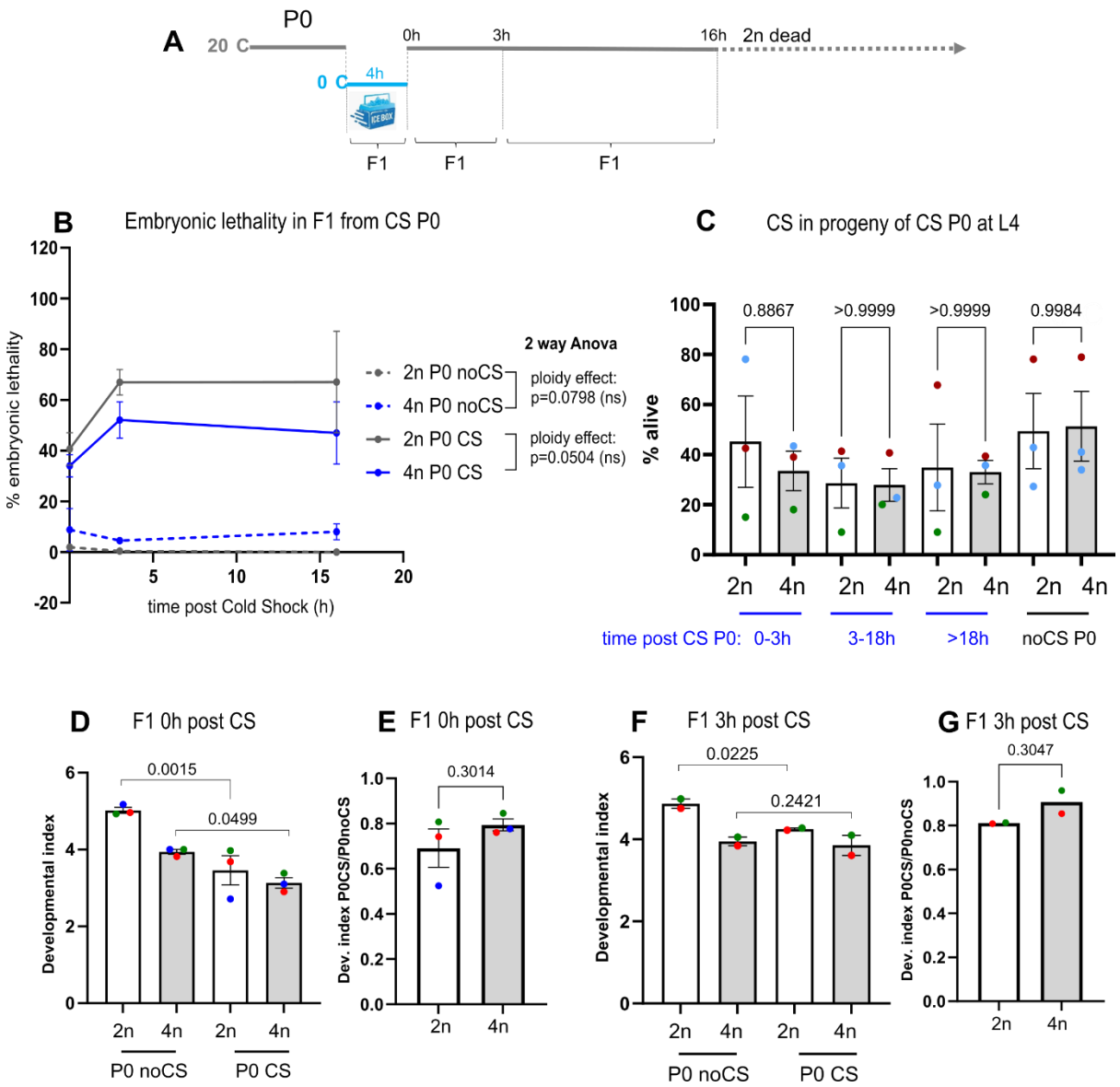
A
P0
20 C
0 C
4h
0h
3h
16h
2n dead
F1
F1
F1
B
Embryonic lethality in F1 from CS P0
% embryonic lethality
time post Cold Shock (h)
2n P0 noCS
4n P0 noCS
2n P0 CS
4n P0 CS
2 way Anova
ploidy effect: p=0.0798 (ns)
ploidy effect: p=0.0504 (ns)
C
CS in progeny of CS P0 at L4
% alive
0.8867
>0.9999
>0.9999
0.9984
time post CS P0: 0-3h
3-18h
>18h
noCS P0
D
F1 0h post CS
Developmental index
0.0015
0.0499
P0 noCS
P0 CS
E
F1 0h post CS
Dev. index P0CS/P0noCS
0.3014
F
F1 3h post CS
Developmental index
0.0225
0.2421
P0 noCS
P0 CS
G
F1 3h post CS
Dev. index P0CS/P0noCS
0.3047

Figure 4.